

Synthesis, Characterization, and Photoisomerization Studies of Azo- and Stilbene-Containing Surfactant Rhenium(I) Complexes

Vivian Wing-Wah Yam,* Yu Yang, Jiaxin Zhang, Ben Wai-Kin Chu, and Nianyong Zhu

Department of Chemistry, The University of Hong Kong, Pokfulam Road, Hong Kong, People's Republic of China

Received March 12, 2001

A series of rhenium(I) surfactant complexes, *fac*-[Re(CO)₃(N–N)(L)]PF₆ (N–N = diimine, L = pyridyl ligand), with various azo- and stilbene-containing ligands have been synthesized and their photophysical properties studied. The X-ray crystal structure of the complex *fac*-[Re(CO)₃(bpy)(L)]PF₆ (bpy = 2,2'-bipyridine, L = 4-(4'-octadecyloxyphenylstyryl)pyridine) has been determined. The photoinduced isomerization processes of these complexes and their free ligands have been studied by electronic absorption and ¹H NMR spectroscopy, and their quantum yields determined.

Introduction

The reversible *trans*–*cis* photoisomerization of azobenzene, stilbene, and their derivatives is of great interest for applications in optical data storage systems.^{1–3} The photoinduced *trans*–*cis* isomerization process in several media has been studied.⁴ Despite numerous reports on the photochemical and photophysical studies of photoisomerizable organic compounds and polymers, only a limited number of investigations on the inorganic/organometallic counterparts with photoisomerizable ligands were reported.^{5–11} Photoinduced isomerization can be achieved by direct irradiation or sensitization via inter- or intramolecular energy transfer processes.

Rhenium(I) tricarbonyl diimine complexes are well known for their rich photophysical and photochemical properties.¹² These complexes, with low-lying MLCT excited states and fairly long lifetimes, have been widely used as photosensitizers for a variety of reactions, including photoisomerization. Early work by Wrighton and co-workers¹³ demonstrated the intermolecular energy transfer from the triplet excited states of the Re(I) complexes to *trans*-stilbene at a diffusion-controlled rate. The spectroscopic *trans*-stilbene triplet was produced which decayed to the characteristic photostationary ratio of *cis*- and *trans*-stilbene.¹³ Later on, intramolecular energy transfer processes from the ³MLCT state to the azo- or stilbene-containing ligands coordinated to the Re(I) metal center have also been systematically studied.^{7a,8,9,12} It was thought that the connection of the photoisomerizable moiety to the Re(I) photosensitizer would shorten the energy transfer pathway and minimize the influence of diffusion.

With our continuous interests in the design of Re(I) tricarbonyl diimine complexes possessing photochromic behavior^{8,14a} and second-order nonlinear optical

* E-mail: wwyam@hku.hk.

(1) (a) Liu, Z. F.; Hashimoto, K.; Fujishima, A. *Nature* **1990**, *347*, 6294. (b) Tachibana, H.; Azumi, R.; Nakamura, T.; Matsumoto, M.; Kawabata, Y. *Chem. Lett.* **1992**, *1*, 173. (c) Maack, J. Ahuja, R. C.; Mobius, D.; Tachibana, H.; Matsumoto, M. *Thin Solid Films* **1994**, *242*, 122.

(2) (a) Natansohn, A.; Xie, S.; Rochon, P. *Macromolecules* **1992**, *25*, 5531. (b) Natansohn, A.; Rochon, P.; Gosselin, J.; Xie, S. *Macromolecules* **1992**, *25*, 2268. (c) Rochon, P.; Gosselin, J.; Natansohn, A.; Xie, S. *Appl. Phys. Lett.* **1992**, *60*, 4.

(3) Ichimura, K.; Seki, T.; Kawanishi, Y.; Suzuki, Y.; Sakuragi, M.; Tamaki, T. *Photoreactive Materials for Ultrahigh-Density Optical Memory*; Irie, M., Ed.; Elsevier: Amsterdam, 1994.

(4) (a) Toutianoush, A.; Tiede, B. *Macromol. Rapid. Commun.* **1998**, *19*, 591. (b) Wang, R.; Iyoda, Y.; Hashimoto, K.; Fujishima, A. *J. Phys. Chem.* **1995**, *99*, 3352. (c) Ikeda, T.; Tsutsumi, O. *Science* **1995**, *268*, 1873. (d) Saremi, F.; Tiede, B. *Adv. Mater.* **1998**, *10*, 388. (e) Enomoto, T.; Hagiwara, H.; Tryk, D. A.; Liu, Z. F.; Hashimoto, K.; Fujishima, A. *J. Phys. Chem. B* **1997**, *101*, 7422. (f) Balzani, V.; Stoddart, J. F.; Williams, D. J. *Chem. Eur. J.* **1999**, *5*, 860.

(5) Wrighton, M. S.; Morse, D. L.; Pdungsap, L. *J. Am. Chem. Soc.* **1975**, *97*, 2073.

(6) Zarnegar, P. P.; Whitten, D. G. *J. Am. Chem. Soc.* **1971**, *93*, 3776. (b) Zarnegar, P. P.; Bock, C. R.; Whitten, D. G. *J. Am. Chem. Soc.* **1973**, *95*, 4367. (c) Whitten, D. G.; McCall, M. T.; Zarnegar, P. P.; Whitten, D. G. *J. Am. Chem. Soc.* **1969**, *91*, 5097.

(7) Shaw, J. R.; Webb, R. T.; Schmehl, R. H. *J. Am. Chem. Soc.* **1990**, *112*, 1117. (b) Shaw, J. R.; Schmehl, R. H. *J. Am. Chem. Soc.* **1991**, *113*, 389.

(8) (a) Yam, V. W. W.; Lau, V. C. Y.; Cheung, K. K. *J. Chem. Soc., Chem. Commun.* **1995**, 1195. (b) Yam, V. W. W.; Lau, V. C. Y.; Wu, L. X. *J. Chem. Soc., Dalton Trans.* **1998**, 1461.

(9) Schanze, K. S.; Lucia, L. A.; Cooper, M.; Walters, K. A.; Ji, H. F.; Sabina, O. *J. Phys. Chem. A* **1998**, *102*, 5577.

(10) (a) Zacharias, P. S.; Ameerunisha, S.; Korupolu, S. R. *J. Chem. Soc., Perkin Trans. 2* **1998**, 2055. (b) Aiello, I.; Ghedini, M.; La Deda, M.; Pucci, D.; Francescangeli, O. *Eur. J. Inorg. Chem.* **1999**, 1367. (c) Lewis, J. P.; Perutz, R. N.; Moore, J. N. *Chem. Commun.* **2000**, 1865. (d) Yutaka, T.; Kurihara, M.; Kubo, K.; Nishihara, H. *Inorg. Chem.* **2000**, *39*, 3438.

(11) (a) Sun, S. S.; Robson, E.; Dunwoody, N.; Silva, A. S.; Brinn, I. M.; Lees, A. J. *Chem. Commun.* **2000**, 201. (b) Sun, S. S.; Lees, A. J. *J. Am. Chem. Soc.* **2000**, *122*, 8956.

(12) (a) Lees, A. J. *Chem. Rev.* **1987**, *87*, 711. (b) Stufkens, D. J.; Vlcek, A., Jr. *Coord. Chem. Rev.* **1998**, *177*, 127. (c) Stufkens, D. J. *Coord. Chem. Rev.* **1990**, *104*, 39. (d) Schanze, K. S.; MacQueen, D. B.; Perkins, T. A.; Cabana, L. A. *Coord. Chem. Rev.* **1993**, *122*, 63. (e) Vites, J. C.; Lynam, M. M. *Coord. Chem. Rev.* **1998**, *169*, 201.

(13) (a) Wrighton, M. S.; Morse, D. L. *J. Am. Chem. Soc.* **1974**, *96*, 998. (b) Giordano, P. J.; Wrighton, M. S. *J. Am. Chem. Soc.* **1979**, *101*, 2888.

(14) (a) Yam, V. W. W.; Ko, C. C.; Wu, L. X.; Wong, K. M. C.; Cheung, K. K. *Organometallics* **2000**, *19*, 1820. (b) Yam, V. W. W.; Lau, V. C. Y.; Wang, K. Z.; Cheung, K. K.; Huang, C. H. *J. Mater. Chem.* **1998**, *8*, 89. (c) Yam, V. W. W.; Wang, K. Z.; Wang, C. R.; Yang, Y.; Cheung, K. K. *Organometallics* **1998**, *17*, 2440. (d) Yam, V. W. W.; Yang, Y.; Yang, H. P.; Cheung, K. K. *Organometallics* **1999**, *18*, 5252.

properties,^{14b,c,d} a series of Re(I) surfactant complexes with azo- and stilbene-containing ligands have been synthesized and their photophysical properties studied. The photoisomerization properties of these complexes have been studied by electronic absorption and ¹H NMR spectroscopy, and their quantum yields determined. The X-ray crystal structure of one of the complexes, *fac*-[Re(CO)₃(bpy)(L)]PF₆ (bpy = 2,2'-bipyridine, L = 4-(4'-octadecyloxyphenylstyryl)pyridine), has also been determined.

Experimental Section

Materials. Pyridine-2-carboxaldehyde (99%, Aldrich) was distilled before use. Re(CO)₅Cl (98%, Strem) was used as received. 4,5-Diazafluoren-9-one,¹⁵ 4-(4'-octadecyloxyphenylazo)aniline,¹⁶ 4-octadecyloxy-4'-stilbenamine,¹⁷ 4-(4'-aminostyryl)pyridine,¹⁸ and *trans*-4-methyl-4'-(2-(4-hydroxyphenyl)vinyl)-2,2'-bipyridine¹⁹ were prepared by literature methods. *trans*-4-(4'-Octadecyloxyphenylazo)pyridine (**L5**), *trans*-4-(4'-octadecyloxy-styryl)pyridine (**L6**), [ClRe(CO)₃(**L5**)] (**5**), and [ClRe(CO)₃(**L6**)] (**6**) were prepared as described previously.^{14d} All solvents for synthesis were of analytical grade and were used without further purification.

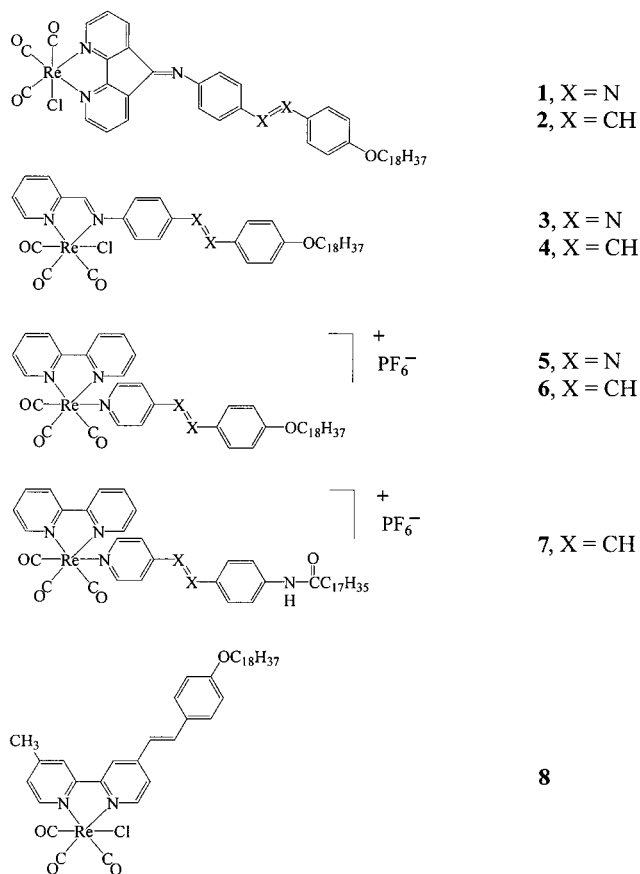
Physical Measurements and Instrumentation. The UV-vis spectra were obtained on a Hewlett-Packard 8452A diode array spectrophotometer, IR spectra as Nujol mulls on a Bio-Rad FTS-7 Fourier transform infrared spectrophotometer (4000–400 cm⁻¹), and steady-state excitation and emission spectra on a Spex Fluorolog-2 111 spectrofluorometer with or without Corning filters. Low-temperature (77 K) spectra were recorded using an optical Dewar sample holder. ¹H NMR spectra were recorded on a Bruker DPX-300 NMR spectrometer with chemical shifts reported relative to tetramethylsilane (Me₄Si). Positive-ion fast-atom bombardment (FAB) and electron-impact (EI) mass spectra were recorded on a Finnigan MAT95 mass spectrometer. Elemental analyses were performed on a Carlo Erba 1106 elemental analyzer at the Institute of Chemistry, Chinese Academy of Sciences in Beijing.

Chemical actinometry was employed for the photochemical quantum yield determination. Incident light intensities were taken from the average values measured just before and after each photolysis experiment using ferrioxalate actinometry.²⁰ The time of irradiation was chosen to monitor 20% or less of the photolysis reaction in order to minimize any effects arising from secondary photolysis.

Syntheses. The structures of Re(I) complexes for photoisomerization studies are given in Scheme 1.

Ligand Syntheses. 9-(4-Octadecyloxy-4'-azobenzenamino)-4,5-diazafluorene (L1). L1 was synthesized by modification of a literature method.²¹ A mixture of 4-(4'-octadecyloxyphenylazo)aniline (0.77 g, 1.65 mmol),

Scheme 1. Structures of Azo- and Stilbene-Containing Surfactant Re(I) Complexes



4,5-diazafluoren-9-one (0.28 g, 1.54 mmol), and 4-toluenesulfonic acid (0.013 g, 0.068 mmol) was dissolved in 20 mL of toluene. The mixture was heated to reflux in an oil bath for 24 h, during which a Dean-Stark apparatus was used to drive the reaction. Most of the solvent was then removed under reduced pressure, and the precipitate formed was filtered. The crude product was purified by recrystallization twice from toluene to give the desired product as a pale yellow solid. Yield: 0.72 g, 74%. Mp: 155 °C. ¹H NMR (300 MHz, CDCl₃, relative to Me₄Si): δ 8.83 (dd, 1H, *J*₁ = 5.0 Hz, *J*₂ = 1.5 Hz, pyridyl H *ortho* to N), 8.66 (dd, 1H, *J*₁ = 4.8 Hz, *J*₂ = 1.5 Hz, pyridyl H *ortho* to N), 8.26 (dd, 1H, *J*₁ = 7.6 Hz, *J*₂ = 1.5 Hz, pyridyl H *para* to N), 8.01 (d, 2H, *J* = 8.6 Hz, aryl H), 7.94 (d, 2H, *J* = 8.9 Hz, aryl H), 7.41 (dd, 1H, *J*₁ = 7.6 Hz, *J*₂ = 5.0 Hz, pyridyl H *meta* to N), 7.13 (d, 2H, *J* = 8.6 Hz, aryl H), 7.04 (m, 4H, pyridyl and aryl H), 4.06 (t, 2H, *J* = 6.5 Hz, -OCH₂-), 1.84 (m, 2H, -CH₂-), 1.49 (m, 2H, -CH₂-), 1.26 (m, 28H, -(CH₂)₁₄-), 0.88 (t, 3H, *J* = 6.6 Hz, -CH₃). UV-vis in CH₂Cl₂, λ/nm (ε × 10⁻⁴/dm³ mol⁻¹ cm⁻¹): 316 (1.72), 362 (3.11), 440 sh (0.83). EI-MS *m/z*: 629 (M⁺). Anal. Calcd for C₄₁H₅₁N₅O: C, 78.18; H, 8.16; N, 11.12. Found: C, 78.57; H, 8.21; N, 11.10.

9-(4-Octadecyloxy-4'-stilbenamino)-4,5-diazafluorene (L2). L2 was synthesized as described for L1

(15) Henderson, L. J., Jr.; Fronczek, F. R.; Cherry, W. R. *J. Am. Chem. Soc.* **1984**, *106*, 5876.

(16) Matsui, M.; Tanaka, N.; Andoh, N.; Funabiki, K.; Shibata, K.; Muramatsu, H.; Ishigure, Y.; Kohyama, E.; Abe, Y.; Kaneko, M. *Chem. Mater.* **1998**, *10*, 1921.

(17) (a) Liu, X. H.; Abser, N.; Bruce, D. W. *J. Organomet. Chem.* **1998**, *551*, 271. (b) Coe, B. J.; Jones, C. J.; McCleverty, J. A.; Bruce, D. W. *Polyhedron* **1993**, *12*, 45.

(18) Peesapati, V.; Rao, U. N.; Pethrick, R. A. *J. Indian Chem. Soc.* **1991**, *68*, 389.

(19) Amoroso, A. J.; Das, A.; McCleverty, J. A.; Ward, M. D.; Barigelletti, F.; Flamigni, L. *Inorg. Chim. Acta* **1994**, *226*, 171.

(20) (a) Parker, C. A. *Proc. R. Soc. London* **1953**, *A220*, 104. (b) Hatchard, C. G.; Parker, C. A. *Proc. R. Soc. London* **1956**, *A235*, 518. (c) Murov, S. L. *Handbook of Photochemistry*; Marcel Dekker: New York, 1973.

(21) Tai, Z. H.; Zhang, G. C.; Qian, X. P.; Xiao, S. J.; Lu, Z. H.; Wei, Y. *Lamgmuir* **1993**, *9*, 1601.

except that 4-octadecyloxy-4'-stilbenamine was used instead of 4-(4'-octadecyloxyphenylazo)aniline. Yield: 0.70 g, 72%. Mp: 173 °C. ¹H NMR (300 MHz, CDCl₃, relative to Me₄Si): δ 8.81 (d, 1H, *J* = 4.9 Hz, pyridyl H *ortho* to N), 8.66 (d, 1H, *J* = 4.1 Hz, pyridyl H *ortho* to N), 8.26 (d, 1H, *J* = 7.0 Hz, pyridyl H *para* to N), 7.58 (d, 2H, *J* = 8.3 Hz, aryl H), 7.47 (d, 2H, *J* = 8.6 Hz, aryl H), 7.40 (dd, 1H, *J*₁ = 7.6 Hz, *J*₂ = 5.0 Hz, pyridyl H *meta* to N), 7.12 (d, 1H, *J* = 16.3 Hz, -CH=CH-), 7.05 (m, 3H, vinyl and pyridyl H), 7.00 (d, 2H, *J* = 8.1 Hz, aryl H), 6.91 (d, 2H, *J* = 8.6 Hz, aryl H), 3.99 (t, 2H, *J* = 6.5 Hz, -OCH₂-), 1.80 (m, 2H, -CH₂-), 1.47 (m, 2H, -CH₂-), 1.26 (m, 28H, -(CH₂)₁₄-), 0.88 (t, 3H, *J* = 6.5 Hz, -CH₃). UV-vis in CH₂Cl₂, λ/nm (ε × 10⁻⁴/dm³ mol⁻¹ cm⁻¹): 314 (3.75), 330 (3.36), 444 (0.44). EI-MS *m/z*: 628 (M⁺). Anal. Calcd for C₄₃H₅₃N₃O: C, 82.25; H, 8.51; N, 6.69. Found: C, 81.90; H, 8.22; N, 6.77.

N-(4-Octadecyloxy-4'-azo)pyridine-2-carbaldimine (L3). L3 was synthesized by modification of a literature method²² by the condensation of pyridine-2-carboxaldehyde (0.128 g, 1.2 mmol) with 4-(4'-octadecyloxyphenylazo)aniline (0.465 g, 1 mmol) for 12 h in refluxing ethanol (100 mL) in the presence of a catalytic amount of glacial acetic acid (0.5 mL). The precipitate formed on cooling was recrystallized from ethanol to give the desired product as a green-yellow solid. Yield: 0.45 g, 81%. ¹H NMR (300 MHz, CDCl₃, relative to Me₄Si): δ 8.74 (d, 1H, *J* = 4.8 Hz, pyridyl H at 6-position), 8.67 (s, 1H, -CH=N-), 8.23 (d, 1H, *J* = 7.9 Hz, pyridyl H at 3-position), 7.96 (d, 2H, *J* = 8.6 Hz, aryl H), 7.92 (d, 2H, *J* = 9.0 Hz, aryl H), 7.84 (td, 1H, *J*₁ = 7.7 Hz, *J*₂ = 1.5 Hz, pyridyl H at 4-position), 7.42–7.38 (m, 3H, pyridyl H at 5-position and aryl H), 7.01 (d, 2H, *J* = 9.0 Hz, aryl H), 4.05 (t, 2H, *J* = 6.5 Hz, -OCH₂-), 1.83 (m, 2H, -CH₂-), 1.48 (m, 2H, -CH₂-), 1.26 (s, 28H, -(CH₂)₁₄-), 0.88 (t, 3H, *J* = 6.6 Hz, -CH₃). UV-vis in CH₂Cl₂, λ/nm (ε × 10⁻⁴/dm³ mol⁻¹ cm⁻¹): 288 (0.88), 378 (3.39). EI-MS *m/z*: 555 (M⁺). Anal. Calcd for C₃₆H₅₀N₄O: C, 77.94; H, 9.08; N, 10.10. Found: C, 77.95; H, 9.38; N, 10.13.

N-(4-Octadecyloxy-4'-styryl)pyridine-2-carbaldimine (L4). L4 was synthesized as described for L3 except that 4-octadecyloxy-4'-stilbenamine was used instead of 4-(4'-octadecyloxyphenylazo)aniline. Yield: 0.39 g, 71%. ¹H NMR (300 MHz, C₆D₆, relative to Me₄Si): δ 8.87 (s, 1H, -CH=N-), 8.51 (d, 1H, *J* = 4.8 Hz, pyridyl H at 6-position), 8.33 (d, 1H, *J* = 7.8 Hz, pyridyl H at 3-position), 7.37–7.31 (m, 4H, aryl H), 7.25 (d, 2H, *J* = 8.4 Hz, aryl H), 7.11–7.01 (m, 2H, pyridyl H at 4-position and -CH=CH-), 6.97–6.90 (m, 3H, -CH=CH- and aryl H), 6.64 (m, 1H, pyridyl H at 5-position), 3.71 (t, 2H, *J* = 6.4 Hz, -OCH₂-), 1.68 (m, 2H, -CH₂-), 1.36–1.42 (m, 30H, -(CH₂)₁₅-), 0.92 (m, 3H, -CH₃). UV-vis in CH₂Cl₂, λ/nm (ε × 10⁻⁴/dm³ mol⁻¹ cm⁻¹): 304 (2.04), 366 (2.43). EI-MS *m/z*: 552 (M⁺). Anal. Calcd for C₃₈H₅₂N₂O: C, 82.56; H, 9.48; N, 5.07. Found: C, 82.36; H, 9.69; N, 4.82.

4-(4'-(N-Octadecylamide)styryl)pyridine (L7). A mixture of stearic acid (0.30 g, 1.03 mmol) and thionyl chloride (0.7 g, 5.88 mmol) was heated to reflux for 2 h, after which the excess thionyl chloride was removed under reduced pressure. Into the oil-like stearoyl chloride-

containing flask was added 4-(4'-aminostyryl)pyridine (0.2 g, 1.02 mmol) in dry benzene (10 mL), and the mixture was heated to reflux for 24 h. After cooling, most of the solvent was removed under reduced pressure. The green-yellow precipitate formed was filtered and redissolved in chloroform and washed with 5% aqueous sodium hydroxide. After evaporation of solvent, the crude product was purified by recrystallization twice from benzene to give the desired product as a pale yellow solid. Yield: 0.35 g, 74%. Mp: 162 °C. ¹H NMR (300 MHz, CDCl₃, relative to Me₄Si): δ 8.56 (d, 2H, *J* = 4.9 Hz, pyridyl H), 7.57 (d, 2H, *J* = 8.6 Hz, aryl H), 7.50 (d, 2H, *J* = 8.7 Hz, aryl H), 7.36 (d, 2H, *J* = 5.9 Hz, pyridyl H), 7.26 (d, 1H, *J* = 16.3 Hz, -CH=CH-), 7.22 (s, 1H, amide), 6.95 (d, 1H, *J* = 16.3 Hz, -CH=CH-), 2.37 (t, 2H, *J* = 7.5 Hz, -CH₂-), 1.74 (m, 2H, -CH₂-), 1.25 (m, 28H, -(CH₂)₁₄-), 0.88 (t, 3H, *J* = 6.7 Hz, -CH₃). EI-MS *m/z*: 462 (M⁺). Anal. Calcd for C₃₁H₄₆N₂O·1/4H₂O: C, 79.69; H, 10.03; N, 5.99. Found: C, 79.91; H, 10.04; N, 5.81.

trans-4-Methyl-4'-(2-(4-octadecyloxyphenyl)vinyl)-2,2'-bipyridine (L8). A mixture of *trans*-4-methyl-4'-(2-(4-hydroxyphenyl)vinyl)-2,2'-bipyridine¹⁹ (0.52 g, 1.8 mmol), 1-bromooctadecane (0.52 g, 1.6 mmol), and K₂CO₃ (0.5 g, 3.6 mmol) was stirred in *N,N*-dimethylformamide (DMF) (10 mL) at ambient temperature for 3 days. Then DMF was removed by distillation under reduced pressure. The residue was redissolved in chloroform (15 mL) and washed with water (3 × 15 mL). The organic layer was separated and dried over anhydrous magnesium sulfate. Filtration and subsequent removal of the solvent by rotary evaporation of the organic solvent yielded the crude product, which was purified by column chromatography on silica gel using chloroform as eluent to afford the desired product. Yield: 0.80 g, 93%. ¹H NMR (300 MHz, CDCl₃, relative to Me₄Si): δ 8.61 (d, 1H, *J* = 5.0 Hz, pyridyl H at 6'-position), 8.57 (d, 1H, *J* = 4.8 Hz, pyridyl H at 6-position), 8.48 (s, 1H, pyridyl H at 3'-position), 8.25 (s, 1H, pyridyl H at 3-position), 7.49 (d, 2H, *J* = 8.6 Hz, aryl H), 7.41 (d, 1H, *J* = 16.3 Hz, -CH=CH-), 7.35 (dd, 1H, *J*₁ = 5.0 Hz, *J*₂ = 1.5 Hz, pyridyl H at 5'-position), 7.15 (d, 1H, *J* = 4.0 Hz, pyridyl H at 5-position), 6.98 (d, 1H, *J* = 16.3 Hz, -CH=CH-), 6.91 (d, 2H, *J* = 8.6 Hz, aryl H), 3.99 (t, 2H, *J* = 6.5 Hz, -OCH₂-), 2.45 (s, 3H, bpy-CH₃), 1.80 (m, 2H, -CH₂-), 1.46 (m, 2H, -CH₂-), 1.26 (m, 28H, -(CH₂)₁₄-), 0.88 (t, 3H, *J* = 6.6 Hz, -CH₃). UV-vis in CH₂Cl₂, λ/nm (ε × 10⁻⁴/dm³ mol⁻¹ cm⁻¹): 288 (2.21), 334 (3.45). EI-MS *m/z*: 540 (M⁺). Anal. Calcd for C₃₇H₅₂N₂O·1/4H₂O: C, 81.49; H, 9.70; N, 5.14. Found: C, 81.37; H, 9.66; N, 4.91.

Syntheses of Re(I) Complexes. Re(I) complexes **1–4** and **8** were prepared by modification of a literature procedure for Re(I) tricarbonyl diimine complexes.^{13a,23} A mixture of Re(CO)₅Cl (54.3 mg, 0.15 mmol) and L (0.15 mmol) in benzene (8 mL) was heated to reflux under N₂ for 2 h. After removal of the solvent, the residue was triply recrystallized from CH₂Cl₂/*n*-hexane. Complex **7** were synthesized as in complexes **5** and **6**,^{14d} from the reaction of [(CH₃CN)Re(CO)₃(bpy)]OTf and the substituted pyridyl ligand **L7**.

(22) Johnson, D. W.; Mayer, H. K.; Minard, J. P.; Banatida, J.; Miller, C. *Inorg. Chim. Acta* **1988**, *144*, 167.

(23) (a) Caspar, J. V.; Meyer, T. J. *J. Phys. Chem.* **1983**, *87*, 952. (b) Dominey, R. N.; Hauser, B.; Hubbard, J.; Dunham, J. *Inorg. Chem.* **1991**, *30*, 4754.

[ClRe(CO)₃(L1)] (1): yellow-brown solid. Yield: 85%. Mp: 186 °C. ¹H NMR (300 MHz, CD₂Cl₂, relative to Me₄Si): δ 8.86 (dd, 1H, *J*₁ = 5.4 Hz, *J*₂ = 0.9 Hz, pyridyl H *ortho* to N), 8.72 (dd, 1H, *J*₁ = 4.2 Hz, *J*₂ = 2.3 Hz, pyridyl H *ortho* to N), 8.47 (dd, 1H, *J*₁ = 7.7 Hz, *J*₂ = 1.0 Hz, pyridyl H *para* to N), 8.06 (d, 2H, *J* = 8.6 Hz, aryl H), 7.96 (d, 2H, *J* = 9.0 Hz, aryl H), 7.72 (dd, 1H, *J*₁ = 7.7 Hz, *J*₂ = 5.5 Hz, pyridyl H *meta* to N), 7.32–7.31 (m, 2H, pyridyl H), 7.22 (d, 2H, *J* = 8.7 Hz, aryl H), 7.06 (d, 2H, *J* = 9.0 Hz, aryl H), 4.08 (t, 2H, *J* = 6.6 Hz, –OCH₂–), 1.85 (m, 2H, –CH₂–), 1.51 (m, 2H, –CH₂–), 1.29 (m, 28H, –(CH₂)₁₄–), 0.90 (t, 3H, *J* = 6.7 Hz, –CH₃). UV–vis in CH₂Cl₂, λ/nm (ε × 10^{–4}/dm³ mol^{–1} cm^{–1}): 324 (2.54), 362 (3.13), 436 (1.06). UV–vis in LB film, λ/nm: 322, 356, 430 sh. IR in Nujol, ν/cm^{–1}: 2041 (s) ν(CO), 1923 (vs) ν(CO), 1864 (s) ν(CO). Positive FAB-MS *m/z*: 936 (M⁺), 901 ({M – Cl}⁺). Anal. Calcd for C₄₄H₅₁ClN₅O₄Re: C, 56.49; H, 5.49; N, 7.49. Found: C, 56.63; H, 5.47; N, 7.48.

[ClRe(CO)₃(L2)] (2): brown solid. Yield: 80%. Mp: 174 °C. ¹H NMR (300 MHz, CDCl₃, relative to Me₄Si): δ 8.85 (dd, 1H, *J*₁ = 5.4 Hz, *J*₂ = 0.9 Hz, pyridyl H *ortho* to N), 8.72 (dd, 1H, *J*₁ = 5.1 Hz, *J*₂ = 1.3 Hz, pyridyl H *ortho* to N), 8.41 (dd, 1H, *J*₁ = 7.7 Hz, *J*₂ = 0.8 Hz, pyridyl H *para* to N), 7.69–7.61 (m, 3H, pyridyl and aryl H), 7.48 (d, 2H, *J* = 8.7 Hz, aryl H), 7.36–7.29 (m, 2H, pyridyl H), 7.16 (d, 1H, *J* = 16.3 Hz, –CH=CH–), 7.08–6.99 (m, 3H, aryl and vinyl H), 6.92 (d, 2H, *J* = 8.7 Hz, aryl H), 3.99 (t, 2H, *J* = 6.6 Hz, –OCH₂–), 1.81 (m, 2H, –CH₂–), 1.47 (m, 2H, –CH₂–), 1.26 (m, 28H, –(CH₂)₁₄–), 0.88 (t, 3H, *J* = 6.7 Hz, –CH₃). UV–vis in CH₂Cl₂, λ/nm (ε × 10^{–4}/dm³ mol^{–1} cm^{–1}): 324 (4.54), 488 (0.76). IR in Nujol, ν/cm^{–1}: 2028 (s) ν(CO), 1921 (vs) ν(CO), 1895 (s) ν(CO). Positive FAB-MS *m/z*: 934 (M⁺), 899 ({M – Cl}⁺). Anal. Calcd for C₄₆H₅₃ClN₃O₄Re: C, 59.18; H, 5.72; N, 4.50. Found: C, 58.96; H, 5.64; N, 4.36.

[ClRe(CO)₃(L3)] (3): yellow-green solid. Yield: 86%. ¹H NMR (300 MHz, CDCl₃, relative to Me₄Si): δ 9.11 (d, 1H, *J* = 4.9 Hz, pyridyl H at 6-position), 8.87 (s, 1H, –CH=N–), 8.13 (m, 1H, pyridyl H at 4-position), 8.03 (m, 3H, pyridyl H at 3-position and aryl H), 7.94 (d, 2H, *J* = 8.9 Hz, aryl H), 7.67 (m, 3H, pyridyl H at 5-position and aryl H), 7.02 (d, 2H, *J* = 9.0 Hz, aryl H), 4.06 (t, 2H, *J* = 6.5 Hz, –OCH₂–), 1.83 (m, 2H, –CH₂–), 1.49 (m, 2H, –CH₂–), 1.26 (m, 28H, –(CH₂)₁₄–), 0.88 (t, 3H, *J* = 6.6 Hz, –CH₃). UV–vis in CH₂Cl₂, λ/nm (ε × 10^{–4}/dm³ mol^{–1} cm^{–1}): 292 (1.08), 378 (2.25), 430 sh (1.24). IR in Nujol, ν/cm^{–1}: 2023 (s) ν(CO), 1915 (s) ν(CO), 1899 (s) ν(CO). Positive FAB-MS *m/z*: 861 (M⁺), 825 ({M – Cl}⁺). Anal. Calcd for C₃₉H₅₀ClN₄O₄Re: C, 54.44; H, 5.86; N, 6.51. Found: C, 54.32; H, 5.87; N, 6.54.

[ClRe(CO)₃(L4)] (4): yellow-green solid. Yield: 87%. ¹H NMR (300 MHz, CDCl₃, relative to Me₄Si): δ 9.09 (d, 1H, *J* = 5.1 Hz, pyridyl H at 6-position), 8.80 (s, 1H, –CH=N–), 8.10 (t, 1H, *J* = 7.1 Hz, pyridyl H at 4-position), 8.00 (d, 1H, *J* = 7.5 Hz, pyridyl H at 3-position), 7.62 (m, 3H, pyridyl H at 5-position and aryl H), 7.52 (d, 2H, *J* = 8.5 Hz, aryl H), 7.48 (d, 2H, *J* = 8.7 Hz, aryl H), 7.14 (d, 1H, *J* = 16.3 Hz, –CH=CH–), 6.99 (d, 1H, *J* = 16.3 Hz, –CH=CH–), 6.91 (d, 2H, *J* = 8.6 Hz, aryl H), 3.99 (t, 2H, *J* = 6.6 Hz, –OCH₂–), 1.80 (m, 2H, –CH₂–), 1.47 (m, 2H, –CH₂–), 1.26 (m, 28H, –(CH₂)₁₄–), 0.88 (t, 3H, *J* = 6.5 Hz, –CH₃). UV–vis in CH₂Cl₂, λ/nm (ε × 10^{–4}/dm³ mol^{–1} cm^{–1}): 308 (2.95), 430

(1.66). IR in Nujol, ν/cm^{–1}: 2017 (s) ν(CO), 1913 (s) ν(CO), 1885 (s) ν(CO). Positive FAB-MS *m/z*: 858 (M⁺), 823 ({M – Cl}⁺). Anal. Calcd for C₄₁H₅₂ClN₂O₄Re: C, 57.36; H, 6.11; N, 3.26. Found: C, 57.72; H, 6.13; N, 3.37.

[Re(CO)₃(bpy)(L7)]PF₆ (7): yellow crystalline solid. Yield: 82%. Mp: 111 °C. ¹H NMR (300 MHz, CDCl₃, relative to Me₄Si): δ 9.09 (d, 2H, *J* = 5.4 Hz, 6,6'-H of bpy), 8.45 (d, 2H, *J* = 8.2 Hz, 3,3'-H of bpy), 8.23 (t, 2H, *J* = 7.6 Hz, 4,4'-H of bpy), 7.97 (d, 2H, *J* = 6.5 Hz, pyridyl H *ortho* to N), 7.73 (t, 2H, *J* = 6.6 Hz, pyridyl H *meta* to N), 7.52–7.47 (m, 3H, 5,5'-H of bpy and amido H), 7.28 (s, 4H, aryl H of L7), 7.14 (d, 1H, *J* = 16.3 Hz, –CH=CH–), 6.65 (d, 1H, *J* = 16.2 Hz, –CH=CH–), 2.37 (t, 2H, *J* = 7.5 Hz, –CH₂–), 1.71 (m, 2H, –CH₂–), 1.24 (m, 28H, –(CH₂)₁₄–), 0.88 (t, 3H, *J* = 6.5 Hz, –CH₃). UV–vis in CH₂Cl₂, λ/nm (ε × 10^{–4}/dm³ mol^{–1} cm^{–1}): 322 (2.54), 370 (4.65). UV–vis in LB film, λ/nm: 324, 366. IR in Nujol, ν/cm^{–1}: 2031 (s) ν(CO), 1937 (s) ν(CO), 1899 (s) ν(CO). Positive FAB-MS *m/z*: 890 (M⁺), 427 ({M – L7}⁺). Anal. Calcd for C₄₄H₅₄F₆N₄O₄Re: C, 51.11; H, 5.26; N, 5.42. Found: C, 51.07; H, 5.17; N, 5.28.

[ClRe(CO)₃(L8)] (8): yellow solid. Yield: 84%. Mp: 155 °C. ¹H NMR (300 MHz, CDCl₃, relative to Me₄Si): δ 8.82–8.79 (m, 2H, pyridyl H at 6,6'-position), 8.12 (s, 1H, pyridyl H at 3'-position), 8.07 (s, 1H, pyridyl H at 3-position), 7.58 (d, 2H, *J* = 8.7 Hz, aryl H), 7.44 (d, 1H, *J* = 16.3 Hz, –CH=CH–), 7.34 (d, 1H, *J* = 6.8 Hz, pyridyl H at 5'-position), 7.22 (d, 1H, *J* = 5.6 Hz, pyridyl H at 5-position), 6.97 (d, 2H, *J* = 8.7 Hz, aryl H), 6.87 (d, 1H, *J* = 16.2 Hz, –CH=CH–), 4.02 (t, 2H, *J* = 6.6 Hz, –OCH₂–), 2.48 (s, 3H, bpy-CH₃), 1.82 (m, 2H, –CH₂–), 1.46 (m, 2H, –CH₂–), 1.26 (m, 28H, –(CH₂)₁₄–), 0.88 (t, 3H, *J* = 6.6 Hz, –CH₃). UV–vis in CH₂Cl₂, λ/nm (ε × 10^{–4}/dm³ mol^{–1} cm^{–1}): 297 (2.46), 367 (2.75), 400 sh (2.43). IR in Nujol, ν/cm^{–1}: 2021 (s) ν(CO), 1916 (vs) ν(CO), 1874 (vs) ν(CO). Positive FAB-MS *m/z*: 847 (M⁺), 812 ({M – Cl}⁺). Anal. Calcd for C₄₀H₅₂ClN₂O₄Re: C, 56.75; H, 6.19; N, 3.31. Found: C, 56.44; H, 6.12; N, 3.08.

Crystal Structure Determination. Crystals of complex **6** were obtained by slow diffusion of diethyl ether vapor into their dichloromethane solution. A yellow crystal of dimensions 0.40 × 0.30 × 0.05 mm mounted on a glass fiber was used for data collection at 28 °C on a MAR diffractometer with a 300 mm image plate detector using graphite-monochromatized Mo-Kα radiation (λ = 0.71073 Å). Data collection was made with a 2° oscillation step of φ, 600 s exposure time, and scanner distance at 120 mm; 100 images were collected. The images were interpreted and intensities integrated using the program DENZO.²⁴ The structure was solved by direct methods employing the SHELXS-97 program²⁵ on a PC. The Re and C atoms were located using the direct method. The other non-hydrogen atoms were found by Fourier synthesis after full-matrix least-squares refinement using the program SHELXL-97²⁵ on

(24) Otwinowski, Z.; Minor, W. *Processing of X-ray Diffraction Data Collected in Oscillation Mode*, Methods in Enzymology, Volume 276: Macromolecular Crystallography; Carter, C. W., Sweet, R. M., Jr., Eds.; Academic Press: New York, 1997; Part A, p 307.

(25) SHELXS97, Sheldrick, G. M. *SHELXS97*. Programs for Crystal Structure Analysis (release 97-2); University of Goettingen: Germany, 1997.

Table 1. Crystal and Structure Determination Data for Complex 6

formula	[C ₄₄ H ₅₅ N ₃ O ₄ Re] ⁺ PF ₆ ⁻
fw	1021.08
<i>T</i> , K	301
<i>a</i> , Å	21.386(2)
<i>b</i> , Å	9.110(1)
<i>c</i> , Å	23.719(2)
α, deg	90
β, deg	100.21(2)
γ, deg	90
<i>V</i> , Å ³	4547.9(8)
cryst syst	monoclinic
space group	<i>P</i> 2 ₁ / <i>a</i>
<i>Z</i>	4
<i>F</i> (000)	2064
<i>D</i> _{calcd} , g cm ⁻³	1.491
abs coeff, mm ⁻¹	2.775
cryst dimens, mm	0.40 × 0.30 × 0.05
λ, Å (graphite monochromated, Mo-Kα)	0.71073
θ range for data collection, deg	0.87 to 25.60
oscillation, deg	2
no. of images collected	100
distance, mm	120
exposure time, s	600
index range	<i>h</i> , -25 to 25; <i>k</i> , -10 to 10; <i>l</i> , -28 to 28
no. of data collected	30264
no. of unique data	8122 [<i>R</i> _{int} = 0.531] ^a
completeness to θ = 25.60°, %	95.1
refin. method	full-matrix least-squares on <i>F</i> ²
no. of data/restraints/params	8122/ 0/ 527
goodness-of-fit on <i>F</i> ²	1.062
final <i>R</i> indices (<i>I</i> > 2σ(<i>I</i>))	<i>R</i> ₁ = 0.0448, <i>wR</i> ₂ = 0.1275
<i>R</i> indices (all data)	<i>R</i> ₁ = 0.0616, <i>wR</i> ₂ = 0.1405
residual extrema in final diff map, e Å ⁻³	0.921 and -1.609

$$^a R_{\text{int}} = \sum |F^2 - F^2(\text{mean})| / \sum [F^2].$$

a PC. One crystallographic asymmetric unit consists of one molecule. In the final stage of least-squares refinement, all non-hydrogen atoms were refined anisotropically. The positions of H atoms generated by the program SHELXL-97 are calculated on the basis of a riding mode with thermal parameters equal to 1.2 times that of the attached C atoms and were included in the calculation of the final *R*-indices.²⁶ Crystal and structure determination data are summarized in Table 1.

Results and Discussion

Syntheses and Characterization. All the Re(I) complexes were synthesized by modification of a literature procedure and characterized by ¹H NMR, IR, and positive-ion FAB-MS and gave satisfactory elemental analyses. These complexes all show three intense IR absorption bands at ca. 1900–2100 cm⁻¹, typical of the tricarbonyl Re(I) moiety in the facial arrangement.^{13b} ¹H NMR spectroscopy showed that the stilbene-contain-

ing complexes are in *trans*-configuration, in which the coupling constant of the two olefinic hydrogens is 16 Hz, typical of that for *trans*-alkenes. The *trans*-configuration of the stilbene unit in complex **6** was further confirmed by X-ray crystallography.

Crystal Structure. The perspective drawing of the complex cation of **6** is shown in Figure 1. Selected bond distances and angles for complex **6** are given in Table 2. The coordination geometry at the Re atom is distorted octahedral with the three carbonyl ligands arranged in a facial fashion, which is similar to that found in other related rhenium(I) systems.¹⁴ The hydrophobic aliphatic chain is running along an axis that is almost perpendicular to the plane containing the Re atom and the bipyridine unit.

Electronic Absorption and Emission Spectroscopy. The electronic absorption spectral and photophysical data of complexes **1–8** are shown in Table 3. The electronic absorption spectra of these complexes in dichloromethane all show an absorption band/shoulder at ca. 370–488 nm at 298 K. With reference to previous work on a related system,¹² this absorption band is tentatively assigned as the dπ(Re) → π*(diimine) metal-to-ligand charge transfer (MLCT) transition. In view of the large extinction coefficient on the order of 10⁴ dm³ mol⁻¹ cm⁻¹, which is much larger by an order of magnitude from the 10³ dm³ mol⁻¹ cm⁻¹ commonly observed for rhenium(I) diimine MLCT transition, as well as the presence of a similar low energy absorption band in the free ligand, it is likely that the lowest energy absorption band in complexes **1–8** would consist of an admixture of intraligand (IL) π → π*(L) and MLCT character. The higher energy absorption band at ca. 292–324 nm is ascribed to the π → π* intraligand (IL) transition, which also occurs in the free ligands.

Upon excitation at λ > 350 nm in degassed dichloromethane solution at ambient temperature, complexes **1** and **5–7** were found to emit weakly (Φ_{lum}(CH₂Cl₂) < 10⁻³), with the emission maxima centered at ca. 530–580 nm (Figure 2), while no emission was detected for complexes **3** and **4**. On the other hand, complex **2** showed a relatively stronger emission (Φ_{lum}(CH₂Cl₂) ≈ 2 × 10⁻³). With reference to previous work on related Re(I) tricarbonyl diimine systems,¹² emissions in fluid solution are suggestive of an origin of a triplet MLCT state. The relatively weaker or lack of emission intensity of complexes **1** and **3–7** with respect to that of **2** may be attributed to the presence of an efficient energy transfer quenching pathway from the ³MLCT state to the ³IL state of the azo or styrylpyridine moiety, which are well-known triplet state energy acceptors. Such an energy transfer process is less facile for complex **2**, since it has a lower-lying ³MLCT state which will be less efficient in transferring its excited state energy to the stilbene acceptor (*E*_T(4-methoxystilbene) = 48.3 kcal mol⁻¹),²⁷ resulting in a stronger emission quantum yield. Similar findings have been reported in related systems.⁸ The emission energies of the complexes in 77 K glass are found to be blue-shifted with respect to that in fluid solution, attributed to the well-known rigidochromic effect, typical of this class of compounds.^{12a,13} In addition, a less intense vibronic-structured band attributed to ³IL emission was observed, which over-

(26) Since the structure refinements are against *F*², *R*-indices based on *F*² are larger than (more than double) those based on *F*. For comparison with older refinements based on *F* and an OMIT threshold, a conventional index *R*₁ based on observed *F* values larger than 4σ(*F*) is also given (corresponding to Intensity ≥ 2σ(*I*)). *wR*₂ = {Σ[w(*F*_o² - *F*_c²)²]/Σ[w(*F*_o²)]^{1/2}}, *R*₁ = Σ||*F*_o - *F*_c||/Σ|*F*_o|. The goodness of fit is always based on *F*²: *GoF* = *S* = {Σ[w(*F*_o² - *F*_c²)²]/(n - p)}^{1/2}, where *n* is the number of reflections and *p* is the total number of parameters refined. The weighting scheme is *w* = 1/[σ²(*F*_o²) + (*aP*)² + *bP*], where *P* is [2*F*_o² + Max(*F*_o², 0)]/3.

(27) Görner, H. *J. Phys. Chem.* **1989**, *93*, 1826.

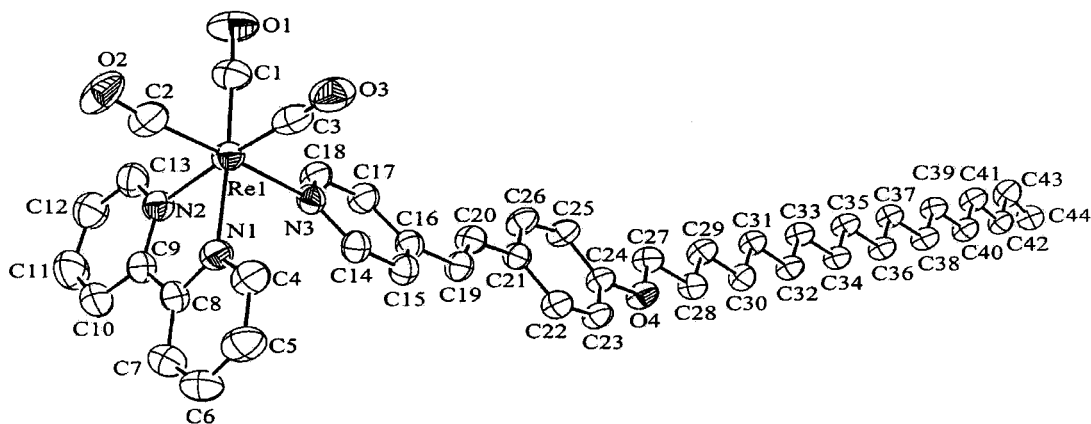


Figure 1. Perspective drawing of the complex cation of **6** with atomic numbering scheme. Hydrogen atoms have been omitted for clarity. Thermal ellipsoids are shown at the 30% probability level.

Table 2. Selected Bond Distances (Å) and Angles (deg) for Complex 6

Distances			
Re(1)–N(1)	2.177(4)	Re(1)–N(2)	2.176(6)
Re(1)–N(3)	2.219(4)	Re(1)–C(1)	1.928(7)
Re(1)–C(2)	1.927(7)	Re(1)–C(3)	1.905(9)
O(1)–C(1)	1.148(7)	O(2)–C(2)	1.143(8)
O(3)–C(3)	1.170(9)	C(19)–C(20)	1.320(8)
Angles			
N(1)–Re(1)–N(2)	75.02(18)	N(1)–Re(1)–N(3)	85.20(15)
N(1)–Re(1)–C(1)	173.7(2)	N(1)–Re(1)–C(2)	94.7(2)
N(1)–Re(1)–C(3)	99.4(2)	N(2)–Re(1)–N(3)	82.45(18)
N(2)–Re(1)–C(1)	98.6(2)	N(2)–Re(1)–C(2)	93.8(3)
N(2)–Re(1)–C(3)	174.4(2)	N(3)–Re(1)–C(1)	93.7(2)
N(3)–Re(1)–C(2)	176.2(3)	N(3)–Re(1)–C(3)	96.9(2)
C(1)–Re(1)–C(2)	85.9(3)	C(1)–Re(1)–C(3)	86.9(3)
C(2)–Re(1)–C(3)	86.9(3)	C(16)–C(19)–C(20)	124.4(5)
C(19)–C(20)–C(21)	128.9(5)		

Table 3. Photophysical Data for Rhenium(I) Tricarbonyl Diimine Complexes 1–8

complex	medium (T/K)	absorption λ /nm ($\epsilon \times 10^{-4}/\text{dm}^3 \text{ mol}^{-1} \text{ cm}^{-1}$)	emission λ /nm ($\tau_0/\mu\text{s}$)
1	CH ₂ Cl ₂ (298)	324 (2.54), 362 (3.13), 436 (1.06)	576 (<0.10)
	glass (77)		526 ^a
2	CH ₂ Cl ₂ (298)	324 (4.54), 488 (0.76)	615 (<0.10)
	glass (77)		536 ^a
3	CH ₂ Cl ₂ (298)	292 (1.08), 378 (2.25), 430 sh (1.24)	<i>b</i>
	CH ₂ Cl ₂ (298)	308 (3.10), 430 (1.66)	<i>b</i>
4	CH ₂ Cl ₂ (298)	322 (1.16), 396 (3.36)	554 (<0.10)
	glass (77)		492 ^a
5	CH ₂ Cl ₂ (298)	324, 388	<i>b</i>
	glass (77)		492 ^a
6	CH ₂ Cl ₂ (298)	320 (1.86), 370 (2.92)	540 (<0.10)
	glass (77)		492 ^a
7	CH ₂ Cl ₂ (298)	324, 366	530
	glass (77)		494 ^a
8	CH ₂ Cl ₂ (298)	324, 366	<i>b</i>
	glass (77)	297 (2.46), 367 (2.75), 400 sh (2.43)	622, 675 ^a

^a In ethanol/methanol (4:1, v/v) glass. ^b Too weak to be measured.

lapped with the more intense ³MLCT band (Figure 2). Complex **8** was found to be nonemissive in solution but emissive in frozen glasses upon excitation. The emission spectrum of complex **8** in 77 K glasses shows vibronic structures with vibrational progression spacings of ca. 1260 cm⁻¹, typical of the ring C–H deformation vibra-

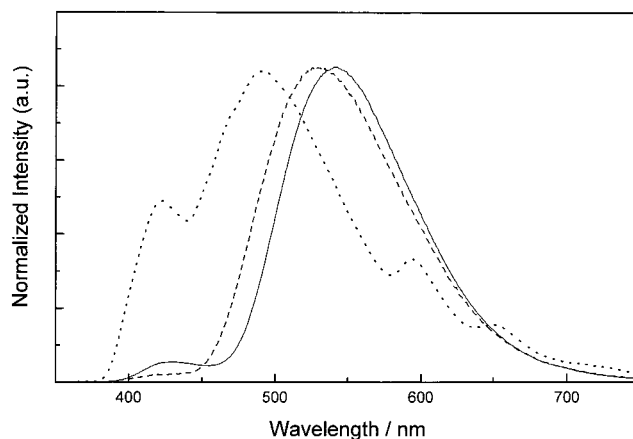


Figure 2. Emission spectra of complex **6** in glass state (---), LB film (···), and CH₂Cl₂ (—).

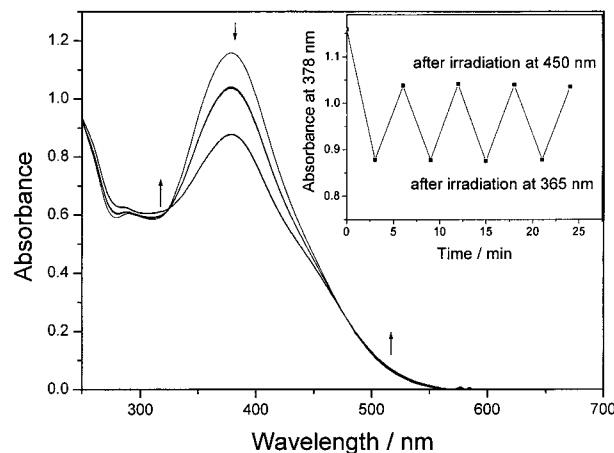


Figure 3. Photoinduced switching of complex **3** between the two photostationary states in degassed CH₂Cl₂. The inset shows the change of the absorbance of complex **3** at 378 nm upon irradiation at $\lambda = 450$ and 365 nm each for 3 min.

tions in the ground state. With reference to the studies of Schmehl and co-workers on the structurally related Re(I) complex [(CO)₃(CH₃CN)Re(mstyb)]PF₆ (mstyb = *trans*-4-styryl-4'-methyl-2,2'-bipyridine)^{7b} where the low-temperature emission was assigned as derived from an ³IL origin, the emission observed in complex **8** in 77 K glass is also believed to originate from an ³IL excited state.

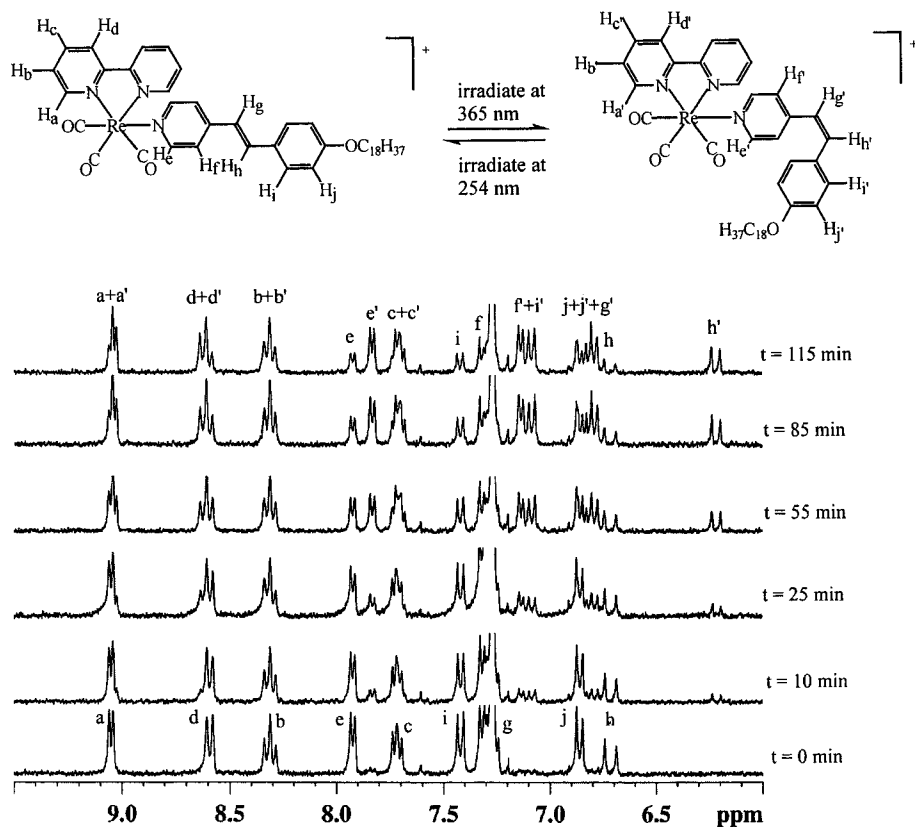


Figure 4. ^1H NMR spectral changes of complex **6** in CDCl_3 at 298 K during the course of irradiation at $\lambda = 365$ nm.

Photoisomerization Reactivity

Electronic Absorption Studies. For the azo-containing complexes **1** and **3** and their free ligands **L1** and **L3**, reversible electronic absorption spectral changes in degassed dichloromethane solution were observed upon alternate irradiation at 365 and 450 nm. Figure 3 shows the electronic absorption changes of complex **3** upon the alternate irradiation at $\lambda = 365$ and 450 nm. Two clean and well-defined isosbestic points at 325 and 478 nm were observed. The spectral changes are suggested to be associated with the *trans*–*cis* isomerization of the $-\text{N}=\text{N}-$ moiety. According to Rau's classification,²⁸ these azo-containing compounds, **1**, **L1**, **3**, and **L3**, are "azobenzene type" in nature and thus are expected to undergo efficient photoisomerization. On the other hand, both complex **5** and its free ligand **L5** showed no obvious electronic absorption changes attributable to the formation of *cis*-isomers after irradiation. It is likely that **L5** with an electron-donating alkoxy substituent on the phenylazopyridine is a poorer energy acceptor, leading to the inefficient photoisomerization reactions of both **L5** and **5**.

For the stilbene-containing complexes, **2**, **4**, and **6–8**, only complexes **6–8** showed reversible electronic absorption spectral changes upon alternate irradiation at $\lambda = 365$ and 254 nm. The intense absorption band centered at ca. 350–380 nm decreases in intensity upon irradiation at $\lambda = 365$ nm and recovers upon irradiation at $\lambda = 254$ nm. These changes are attributed to the *trans*–*cis* isomerization of the $-\text{CH}=\text{CH}-$ moiety. Their corresponding free ligands, **L6**, **L7**, and **L8**, also showed

similar electronic absorption changes upon irradiation at the different wavelengths. The lack of photoisomerization in complexes **2** and **4** may be attributed to the presence of an effective thermal back-reaction as well as an inefficient intramolecular energy transfer pathway from the $^3\text{MLCT}$ to the ^3IL state, as is reflected by the intense emission observed for complexes **2** and **4**.

It is also worthy to note that photoisomerization of complex **8** occurred even upon irradiation into the predominantly MLCT band at $\lambda = 480$ nm, while no photoisomerization was observed for the free ligand **L8** upon irradiation at such a low-energy region. It was proposed that the presence of an efficient photosensitization pathway, i.e., intramolecular energy transfer from the $^3\text{MLCT}$ state to the ^3IL , would be responsible for such observations. It is clear that introduction of the Re metal center made it possible to apply visible light for the photoisomerization of stilbene-containing compounds.

LB films of the azo- or stilbene-containing complexes, **1**, **5**, and **7**, were also subjected to photoisomerization studies; however, no obvious electronic absorption change was observed. It is well known that the cross-sectional area of the *cis*-isomer is much larger than that of the *trans*-isomer; thus free volume is necessary for the molecules to isomerize. In our systems, the LB films obtained show close-packed arrangements in the solid phase with not much free volume, and as a result it is not surprising to find that the photoisomerization process is prohibited in LB films.

^1H NMR Studies. The photoisomerization process of the stilbene-containing complexes could be monitored by ^1H NMR spectroscopy due to the fact that the chemical shifts and coupling constants of the protons,

(28) Rau, H. In *Photochemistry and Photophysics*; Rebek, J. F., Ed.; Boca Raton, FL, 1990; Vol. II, Chapter 4.

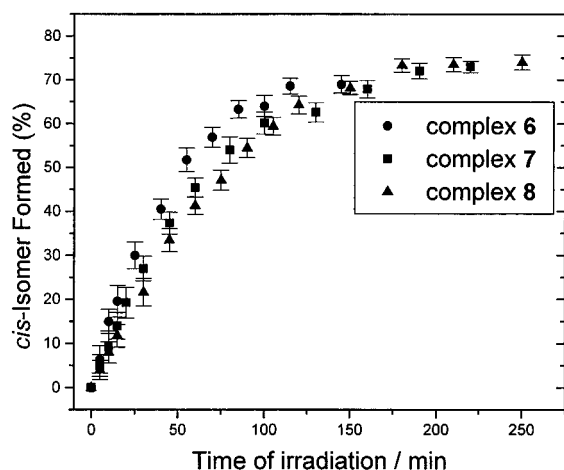


Figure 5. Plots of the percentage yield of the *cis*-isomer formed against the time of irradiation at $\lambda = 365$ nm.

Table 4. Quantum Yields for the Photoisomerization Process of Complexes 6–8 and Their Corresponding Free Ligands upon Excitation at $\lambda = 365$ nm

compound	quantum yield, $\phi_{trans-cis}$	<i>cis</i> -isomer formed (%) in photostationary state
6	0.49	69
7	0.43	72
8	0.42	73
L6	0.50	81
L7	0.48	83
L8	0.48	89

especially the olefinic protons, in the two configurations are fairly different. Generally, the chemical shift in *trans*-alkenes is downfield relative to that of *cis*-alkenes, with a coupling constant of 16 Hz for the *trans*-form and 12 Hz for the *cis*-form. The ^1H NMR spectral changes during the course of the photoinduced isomerization reaction are illustrated in Figure 4. A dependence of the yield of the *cis*-isomer formed of complexes **6–8** on the irradiation time is shown in Figure 5. Upon irradiation at $\lambda = 365$ nm, the amount of *cis*-isomer formed increased gradually, with a concomitant decrease in the amount of *trans*-isomer until a photostationary state was reached. For example, for complex **6**, a photostationary state of $69 \pm 2\%$ *cis*-isomer and $31 \pm 2\%$ *trans*-isomer was achieved upon irradiation of the pure *trans*-isomer (Figure 5).

Quantum Yield Studies. To obtain a quantitative measure of the photoinduced isomerization processes of the rhenium(I) diimine complexes, the photochemical quantum yield for the *trans*–*cis* isomerization process

of the complexes was determined using chemical actinometry. Incident light intensities were taken from the average values measured just before and after each photolysis experiment using potassium ferrioxalate actinometry.²⁰ In the present study, stilbene-containing complexes were chosen instead of azo-containing complexes, as the photoisomerization process of stilbene-containing complexes could be readily monitored by ^1H NMR spectroscopy. A control experiment to correct for the presence of any thermal *trans*–*cis* isomerization was performed in each case, in which an equal amount of the compound was dissolved in the same amount of deuterated chloroform and placed in the dark. A real-time monitoring of the thermal control by ^1H NMR spectroscopy was performed in each case, from which no observable *cis*-isomer was formed in the absence of light. The quantum yields of the photochemical reactions are summarized in Table 4. The slightly lower quantum yields of the complexes relative to that of their corresponding free ligands may be a result of the involvement of the larger steric bulk associated with the metal complexes.

Conclusion

A series of Re(I) tricarbonyl diimine complexes with various azo- and stilbene-containing ligands have been designed and successfully synthesized. Upon alternate irradiation at different wavelengths, the complexes with photoisomerizable ligands would undergo reversible photoisomerization, which could be readily monitored by electronic absorption and ^1H NMR spectroscopy. Although the photochemical reaction quantum yields of the complexes are slightly lower than that of the free ligands, the introduction of the Re(I) metal center presents an efficient photosensitization pathway, i.e., intramolecular energy transfer from the $^3\text{MLCT}$ state to the ^3IL , and thus made it possible to apply visible light for the photoisomerization of this kind of compound.

Acknowledgment. V.W.-W.Y. acknowledges financial support from the Research Grants Council and The University of Hong Kong and the receipt of a Croucher Senior Research Fellowship from the Croucher Foundation. Y.Y. acknowledges the receipt of a part-time demonstratorship, J.Z. the receipt of a Postgraduate Studentship, and B.W.K.C. and N.Z. the receipt of University Postdoctoral Fellowships, all of which are administered by The University of Hong Kong.

OM010192M